Electronic Supplementary Material (ESI) for Nanoscale Horizons.
This journal is © The Royal Society of Chemistry 2017

Electronic Supplementary Information

Nematic structuring of transparent and multifunctional nanocellulose papers

M. Zhao, F. Ansari, M. Takeuchi, M. Shimizu, T. Saito, L. A. Berglund* and A. Isogai*

*E-mail: asaitot@mail.ecc.u-tokyo.ac.jp (T.S.), blund@kth.se (L.B.)

This file includes Experimental methods, Figures S1−S3, and Tables S1−S2.

Experimental methods

Preparation of CNF Dispersions. Undried softwood bleached kraft pulp (1 g by dry weight), supplied by Nippon Paper Industries, was chemically modified by the TEMPO (0.1 mmol)/NaBr (1 mmol)/NaClO (3.8 mmol) oxidation in water (100 mL) at pH 10.[1] The pulp was further treated with $NaBH_4$ (0.1 g) in water (100 mL) at pH10 to eliminate unstable aldehyde groups remaining in the pulp.[2] The carboxylate content of the resulting pulp was 1.2 mmol/g. The pulp (0.1 g by dry weight) was suspended in water (100 mL), mechanically disintegrated using a Physcotron NS-56 (Microtec, Japan) equipped with a 20 mm-diameter shaft at 7500 rpm for 6 min, and sonicated using a US-300T (Nihon Seiki, Japan) equipped with a 26 mm-diameter tip at 70% output for 8 min. The unfibrillated fraction (~30%) was separated by centrifugation at 12,000*g* for 10 min, and the supernatant was collected as a CNF dispersion. The 0.07% dispersion was concentrated to 0.1% using an evaporator, and then stored in a refrigerator before use. The average widths and lengths of the resulting CNFs were approximately 3 nm and 1 μm, respectively.

Preparation of NO films. The 0.1% CNF dispersion was concentrated to 0.4% using an evaporator. The 0.4% CNF dispersion (80 mL) was poured into a 90-mm-diameter polystyrene petri dish and dried at rest in an oven at 40 °C for 1 week. The resulting film was then conditioned at 23 °C and 50% RH for more than 2 days. The edge part of the film was cut into a square with dimensions of 5 × 5 cm^2.

Preparation of RO films. The 0.1% CNF dispersion (200 mL) was diluted with distilled water (100 mL). Then, a 0.4 M NaCl solution (100 mL) was slowly added to the dispersion to prevent nematic ordering of the CNFs; for reference, a photograph of a 0.4% CNF dispersion including 0.1 M NaCl placed between crossed polarizers is shown in Supplementary Figure S4, revealing no nematic ordering of the CNFs with NaCl. The 0.05% CNF dispersion containing 0.1 M NaCl (400 mL) was vacuum-filtered using a membrane filter with a pore size of 0.65 μm (DVPP, Millipore) for 8 h to form a stiff gel film (CNF retention on the filter: > 99%). After adding a sufficient amount of distilled water (400 mL), the gel film was further vacuum-filtered for 30 h to rinse away any NaCl remaining in the gel. The purified gel film with a thickness of approximately 1 mm and a diameter 75 mm was carefully peeled from the filter, and transferred onto an acrylic plate. The edge of the gel film was fixed on the plate with cellophane tape and dried in an oven at 40 °C for 2 days. The resulting film was conditioned and cut into a square in the same manner as for the NO films.

Preparation of NO-RO Intermediate Strucrures. The 0.1% CNF dispersion (200 mL) was directly vacuum-filtered for 12 h in the same manner as for the RO films, resulting in the formation of a gel film with a thickness of approximately 1 mm. The gel film was also dried, conditioned, and cut in the same manner as for the RO films. A birefringence image of the 0.1% dispersion is shown in Supplementary Figure S5, revealing the nematic ordering of dispersed CNFs to some extent even at a low concentration of 0.1%. The 0.1% dispersion exhibited sufficiently low viscosity for vacuum-filtration processing, while enabling the nematic ordering of the CNFs.

TEM Analysis. A CNF film was soaked in 30% ethanol for 3 h and gradually dehydrated by solvent exchanging with 50–100% ethanol. The dehydrated film was then soaked in propylene oxide for 30 min, followed by solvent exchanging with propylene oxide solutions including an epoxy resin (Epon 812) at ratios of 1:2, 1:1, and 2:1 sequentially at intervals of 4 h. The film was finally embedded in a neat epoxy resin for 4 h and cured at 60 °C for 1 day. The resin-embedded film was sectioned at an angle of 45° relative to the film plane using a Leica Ultracut-E microtome equipped with a diamond knife. The resulting 80-nm-thick section was stained with a water/ethanol (1:1) mixed solution of 2% uranyl acetate for 10 min and then with a Reynolds solution of 2% lead citrate at pH 12 for 30 min. The stained section was examined using a JEOL JEM-2000EX microscope at 200 kV.

SEM Analysis. A CNF film was frozen in a liquid nitrogen bath, and fractured in situ by bending. The freeze-fractured surface was settled at room temperature with blowing of dry nitrogen gas, and treated using a Meiwafosis Neoc osmium coater at 6 mA for 2.5 s. The osmium-treated surface was examined using a Hitachi S-4800 field-emission microscope at 1.5 kV. The tensile-fractured surface was also osmium-treated and examined in the same manner as the freeze-fractured surface.

XRD Analysis. XRD diagrams of CNF films were recorded on Fujifilm imaging plates in vacuum using a Rigaku Rotaflex RU-200BH (Ni-filtered CuKα) at 100 mA and 50kV. The films were set either parallel or perpendicular to the X-ray beam, and the distances from the imaging plates were calibrated with NaF. The orientation index *f* was calculated from the azimuthal profile of the 200 reflection using the following equation:

$$f = \frac{180° - FWHM}{180°}$$

where *FWHM* is the full width at half maximum.

Structural Profiles of Films. The film thicknesses were measured at 10 different spots for each film using a micrometer at 23 °C and 50% RH. The bulk densities were calculated from their volumes and weights at 23 °C and 50% RH. The moisture contents were calculated from the film weights at 23 °C and 50% RH and those after drying at 105 °C for 3 h. The porosities were calculated using the following equation:

$$Porosity = 1 - \frac{Bulk\ density \times (1 - Moisture\ content)}{1.6}$$

where the constant 1.6 is the true density of the CNFs measured using a BELPycno helium pycnometer.[3] The root-mean square roughness R_q values were measured at 5 different spots with planar dimensions of 10 × 10 μm^2 for each film by tapping mode AFM using a Bruker MultiMode 8 equipped with a NanoScope V controller and a ScanAsyst-Air probe.

Physical Properties of Films. Tensile tests were conducted using a Shimadzu EZ-SX at 23 °C and 50% RH. Approximately 5–8 tensile specimens with widths and lengths of 3 and 30 mm, respectively, were cut out from a single film; in total, approximately 20 specimens were prepared from 3 films for each film type. The gauge length and head speed were set to 10 mm and 1 mm min^{-1}, respectively. The light transmittances were measured at three different spots for each film using a JASCO V-670 spectrophotometer with a beam diameter of 2 mm without an integrating sphere. The oxygen gas permeability was assessed for an area of 5 cm^2 for each film using a MOCON OX-TRAN 2/21 at 23 °C and 50% RH according to ASTM D3985 standard. The thermal diffusivities α in the out-of-plane direction were measured at 10 different spots for each film using thermal wave analysis with an ai-Phase Mobile 1u at 23 °C and 50% RH. The applied voltage was 0.8 V, and the delay in phase of the temperature wave (amplitude of approximately ±0.5 °C) was measured at 10 points within a range of 6−60 Hz for each film spot. The integration time for each point was typically 10 s. During the measurement, the entire device was covered with an optically opaque windshield. The thermal conductivities k were calculated from the diffusivities α using the following equation:

$k = \alpha c \rho$

where c is the specific heat capacity (0.9 J g^{-1} K^{-1}),[3] and ρ is the bulk density. The electrical resistivity was assessed using a Loresta-GX MCP-T700 with a PSP probe at 23 °C and 50% RH according to standard JIS-K-7194. For each film type, two specimens with planar dimensions of 1 × 1 cm^2 were cut out from two films, respectively. The resistance R values were measured at 5 different spots for each specimen (10 spots for each film type). The electric current and measurement time for each spot were 0.1 μA and 30 s, respectively. The surface resistivity ρ_s values (Ω per square) were calculated from the resistance R values using the following equation:

$\rho_s = R \times RCF$

where RCF is a resistivity correction factor that depends on the specimen shape and dimensions and was 3.891 for all the specimens.

Supplementary Figures and Tables

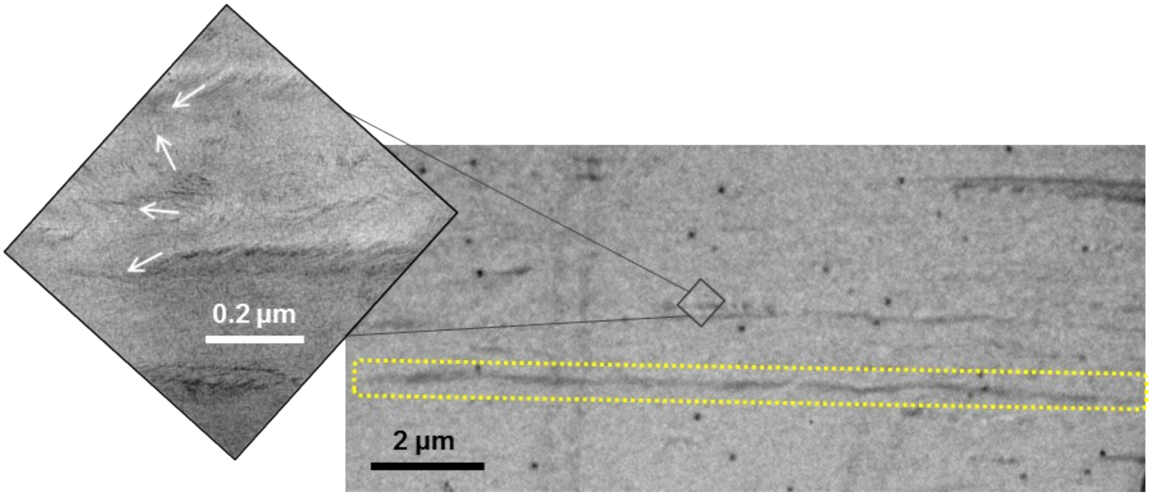

Figure S1. TEM image of the 45° cross-section of the evaporation-condensed film at a low magnification. The yellow dotted line surrounds a single layered domain of oriented CNFs.

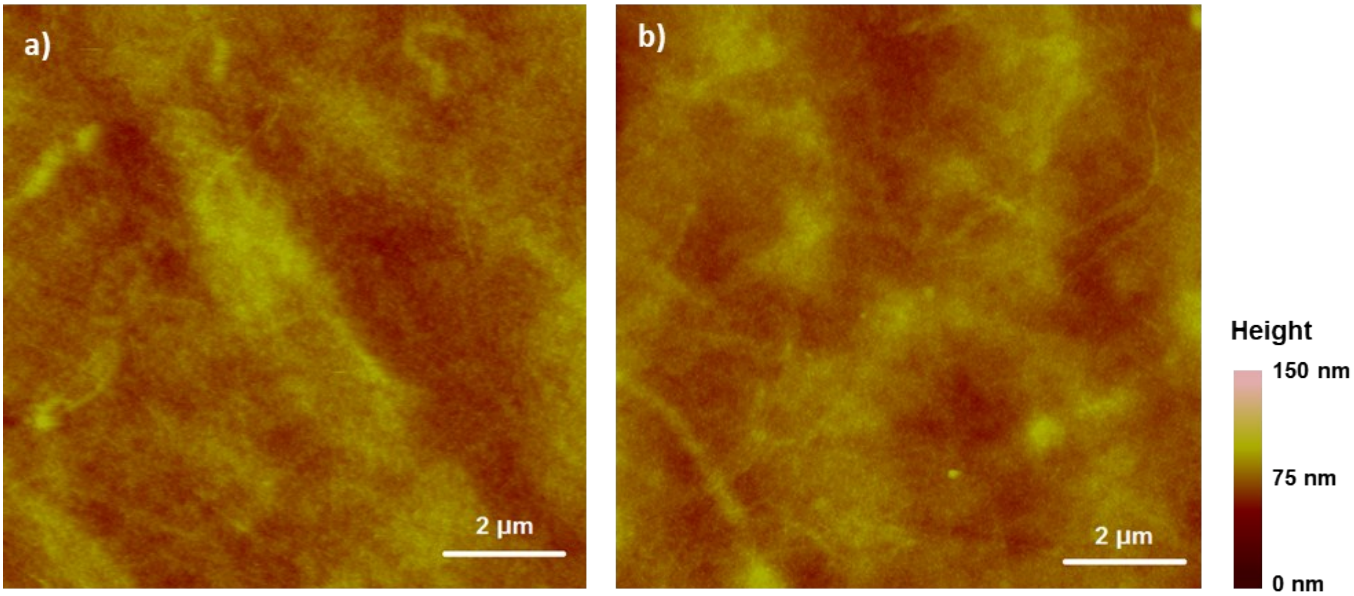

Figure S2. AFM images of the film surfaces of (a) NO and (b) RO films.

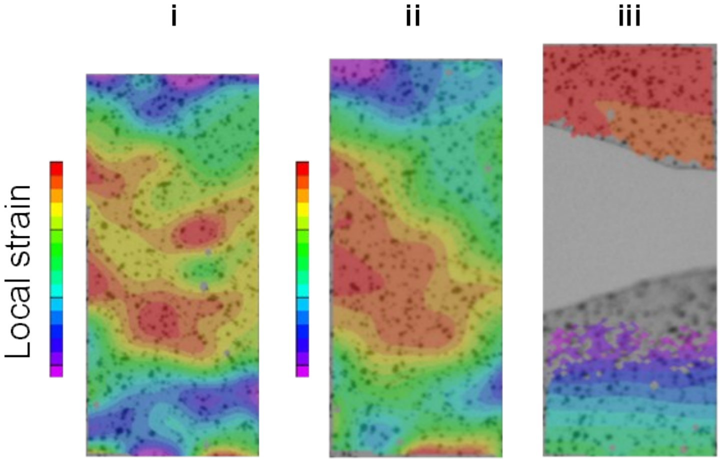

Figure S3. The in-plane strain fields for the plastic deformation of a NO film at the average strains of (i) 1.6%, (ii) 5.5%, and (iii) at breaking.

Figure S4. Photograph of the 0.4% CNF dispersion including 0.1 M NaCl placed between crossed polarizers.

Figure S5. Birefringence image of the 0.1% CNF dispersion at rest. The birefringence is much less than that of the 0.4% dispersion (the inset of Figure 1a), but indicates a distinct ordering.

Table S1. Structural Profiles of NO-RO Intermediate Films at 23 °C and 50%RH

Thickness (μm)	Surface roughness R_q (nm)	Bulk density (g cm^{-3})	Moisture content (%)	Porosity (%)
31.4 ± 1.2	7.7 ± 0.8	1.48	10.0	13.8

Table S2. Material Properties of NO-RO Intermediate Films at 23 °C and 50%RH

Tensile properties:	
Young's modulus E (GPa)	13.6 ± 0.3
yield stress σ_y (MPa)	144 ± 4.4
tensile strength σ_b (MPa)	346 ± 26
elongation at break ε_b (%)	6.5 ± 0.9
Light transmittance at 600 nm (%)	82.4 ± 0.5
Oxygen gas permeability (mL μm m^{-2} day^{-1} kPa^{-1})	0.49

Reference

1. T. Saito, Y. Nishiyama, J. L. Putaux, M. Vignon and A. Isogai, *Biomacromolecules*, 2006, **7**, 1687.
2. S. Takaichi, T. Saito, R. Tanaka and A. Isogai, *Cellulose*, 2014, **21**, 4093.
3. K. Sakai, Y. Kobayashi, T. Saito and A. Isogai, *Sci. Rep.*, 2016, **6**, 20434.